**PASJ:** Publ. Astron. Soc. Japan **62**, 1025–1033, 2010 August 25


# Water Production Rate of the Jupiter-Family Comet 46P/Wirtanen in the 2008 Apparition with the Subaru Telescope/IRCS

Hitomi KOBAYASHI and Hideyo KAWAKITA
*Department of Physics, Faculty of Science, Kyoto Sangyo University,*
*Motoyama, Kamigamo, Kita-ku, Kyoto 603-8555*
*h_kobayashi@cc.kyoto-su.ac.jp*

(Received 2009 December 30; accepted 2010 May 12)

**Abstract**

We present the water production rate of comet 46P/Wirtanen in its 2008 apparition, determined from high-dispersion near-infrared spectroscopic observations. Comet 46P/Wirtanen, one of Jupiter-family comets, was the target of the ROSETTA mission in the past. Observations of comet 46P were carried out in the middle of 2008 February with the Subaru telescope and Infrared Camera and Spectrograph (IRCS) instrument. We detected three water emission lines, and the water production rate was determined to be $(1.7 \pm 0.2) \times 10^{28}$ molecules $s^{-1}$ on 2008 February 19 near the perihelion passage of the comet. This was the first direct detection of water in the coma of comet 46P. We compared our result with the water production rate determined from radio observations near the perihelion passage in the same apparition, and we found that the rate of radio observations is consistent with our value within $\pm 2\sigma$ errors. We also compared the water production rates observed in the 2008 apparition with other results observed in the 1997 apparition. We found that the water production rates in 2008 are consistent with those in 1997. There was no secular change of water production rates around its perihelion passage in recent decades for comet 46P.

**Key words:** comets: general — comets: individual (46P/Wirtanen) — techniques: spectroscopic

## 1. Introduction

The target of this work, comet 46P/Wirtanen, is one of Jupiter-family comets (orbital period $\sim 5.5$ yr). The nature of Jupiter-family comets is not well characterized, in contrast with the Oort cloud comets (the number of Jupiter-family comets observed in detail is smaller than that of the Oort cloud comets) because the Jupiter-family comets are intrinsically fainter than the Oort cloud comets, except for extreme cases (a close approach of the Jupiter-family comets to Earth, such as 73P/Shwassmann–Wachmann 3). In general, telescopes with larger apertures are necessary to the accurate observation of Jupiter-family comets.

Comet 46P was the target of the ROSETTA mission operated by European Space Agency (ESA) in the past, and many studies had been delivered, especially in the 1997 apparition (note that the target of the ROSETTA mission had been changed to comet 67P/Churyumov–Gerasimenko after the observing campaign of comet 46P/Wirtanen in the 1997 apparition because of a delay in the launch schedule). The physical properties of this comet were determined by many different observations, such as the size of nucleus ($\sim 0.6$ km on the assumption of a spherical nucleus, Lamy et al. 1998), the rotational period ($6.0 \pm 0.3$ hr, Lamy et al. 1998), $Af\rho$ as an indicator of dust production (Lamy et al. 1998; Farnham & Schleicher 1998; Fink et al. 1998; Schulz et al. 1998; Stern et al. 1998; Jockers et al. 1998), chemical compositions in the coma (Farnham & Schleicher 1998; Fink et al. 1998; Schulz et al. 1998; Stern et al. 1998), and water production rates (Farnham & Schleicher 1998; Fink et al. 1998; Stern et al. 1998; Bertaux et al. 1999; Crovisier et al. 2002). We focus on the water production rates of comet 46P in this article.

Water is the most abundant species in cometary ice and important as a baseline of the chemical abundance ratios in comets (e.g., Bockelée-Morvan et al. 2004). However, before the middle of the 1990s, it was difficult to observe cometary water directly unless using an airborne observatory (e.g., Kuiper Airborne Observatory) or a space observatory (e.g., Infrared Satellite Observatory), because cometary water emissions are severely absorbed by the telluric water vapor. Thus, the water production rates have been indirectly determined based on the measurements of emission (or absorption) by the OH radical, H atom, or O atom (forbidden oxygen lines) in the coma. These are the photodissociation products of water (or OH) observed in the UV and optical regions, and in radio domain (e.g., A'Hearn et al. 1995; Mäkinen et al. 2001; Crovisier et al. 2002). In the past 10 yr, thanks to the developing instruments and devices, by near-infrared high-dispersion spectroscopic observations could we observe the "hot-band" emissions of water in comets (Dello Russo et al. 2004, 2005). To date, however, there are no reports on the water production rate in comet 46P based on direct measurements of water in the cometary coma.

Here, we report the measurements of water hot-band emission lines in comet 46P/Wirtanen, and also present its water production rate, based on near-infrared spectroscopic observations of water in the comet. In section 2, we introduce our observations and data analysis. In sections 3 and 4, we describe about our results of the water production rate and discuss comparisons of the water production rates observed in the 2008 apparition with those in the 1997 apparition.

**Fig. 1.** Two-dimensional spectrum of comet 46P/Wirtanen observed with the Subaru telescope/IRCS (sky subtracted, and flat-fielded). The horizontal and vertical axes correspond to the dispersion (wavelength) axis and the slit direction, respectively. The positive (white) and negative (black) signals are for A- and B-beams (see section 2). No clear continuum has been detected in the spectrum. Water emission lines are seen in the left side of the figure (pointed by arrows).

**Table 1.** Measured water emission lines and relevant $g$-factors.*

| Line assignment $(\nu_1',\nu_2',\nu_3')J'_{K_a'K_c'}$–$(\nu_1'',\nu_2'',\nu_3'')J''_{K_a''K_c''}$ | Wavenumber [cm$^{-1}$] | Wavelength [Å] | Flux [W m$^{-2}$] | $g$-factor [W molecule$^{-1}$] | Transmittance | Production rate [molecules s$^{-1}$] | Ortho/Para |
|---|---|---|---|---|---|---|---|
| $(101)2_{02}$–$(100)3_{03}$ | 3526.55 | 28356.37 | $(2.08\pm0.31)\times10^{-19}$ | $2.61\times10^{-26}$ | 0.12 | $(1.7\pm0.2)\times10^{28}$ | Ortho |
| $(101)2_{11}$–$(100)3_{12}$ | 3514.41 | 28454.28 | $(1.02\pm0.30)\times10^{-19}$ | $2.52\times10^{-26}$ | 0.39 | $(1.7^{+0.3}_{-0.2})\times10^{28}$ | Ortho |
| $(101)3_{03}$–$(100)4_{04}$ | 3507.27 | 28512.20 | $(4.57\pm2.90)\times10^{-20}$ | $8.72\times10^{-27}$ | 0.66 | $(1.7^{+1.7}_{-0.7})\times10^{28}$ | Para |

* The rest wavenumber and rest wavelength are shown in the 2nd and 3rd columns, respectively. The $g$-factor (for $T_{\rm rot} = 29$ K and $OPR = 3.0$) listed here is corrected by atmospheric transmittances.

## 2. Observations and Data Analysis

Our observations of comet 46P/Wirtanen were performed on 2008 February 17, 18, and 19 UT. We used a high-dispersion echelle spectroscopic mode of the IRCS (Infrared Camera and Spectrograph: Kobayashi et al. 2000) mounted on the Subaru telescope atop Mauna Kea, Hawaii. We used a $0\farcs27 \times 9\farcs37$ slit ($\lambda/\Delta\lambda \sim 10000$ in $L$-band) for the comet and a $0\farcs54 \times 9\farcs37$ slit for a photometric standard star (BS 937, spectral type G0V). Here, we concentrate on observations on February 19 because the humidity was too high (too low transmittances) to detect emission lines from the comets in the near-infrared on both February 17 and 18. The heliocentric and geocentric distances and the relative velocity of the comet to the observers were 1.08 AU, 0.92 AU, and 0.82 km s$^{-1}$ on February 19, respectively. We put the targets (both the comet and the standard star) at two different positions on the slit (A- and B-positions, separated by 5″) and moved from A-position to B in the A-B-B-A sequences. We cycled the A-B-B-A sequences to cancel the sky emissions in the data reduction (see below).

The obtained data were reduced by using the IRAF software package.[1] We calculated ("image A" − "image B") − ("image B" − "image A") (= 2 × "image A" − 2 × "image B") to cancel the sky emission (dark components were also canceled out), and then all results were flat-fielded. A wavelength calibration was performed by comparing background sky emission lines. The two-dimensional spectrum is shown in figure 1.

[1] The Image Reduction and Analysis Facility (IRAF) is distributed by the National Optical Astronomy Observatories, which are operated by the Association of Universities for Research in Astronomy, Inc., under cooperative agreement with the National Science Foundation.

The one-dimensional spectrum centered on the nucleus was extracted from the area corresponding to 9 pixels in a row [$0\farcs27 \times 0\farcs49$ (180 km × 327 km) on the sky]. Usually, the signal from the comet includes both reflected sunlight by cometary dust grains and emission lines from gaseous species in the coma. Therefore, the dust component has to be subtracted in order to extract only the gas emission lines. However, as can be seen in figure 1, no continuum component is recognized in the observed spectra. Thus, we decided to skip subtracting the dust component in the case of comet 46P. There were some reports on the high gas-to-dust ratio in comet 46P (Lamy et al. 1998; Farnham & Schleicher 1998), which are consistent with our observations shown in figure 1. We consider that skipping continuum subtraction does not have a great influence on our conclusion.

Then, the obtained spectrum was flux-calibrated by comparing the observed spectra with those of a standard star, and the result was corrected for the Doppler-shift by the topocentric velocity of the comet at the observations. Additional details of our data-reduction methods are given elsewhere (Kobayashi et al. 2007; Kobayashi & Kawakita 2009). The obtained one-dimensional spectrum is shown in figure 2. We detected three emission lines of hot-band $H_2O$ in our spectrum (figure 2). We list the measurements of fluxes and corresponding transitions of these emission lines in table 1.

## 3. Results

Based on the calibrated spectrum, we determined the water production rate, $Q(H_2O)$ [molecules s$^{-1}$], using the fluorescence-excitation model of $H_2O$ (Dello Russo et al. 2004, 2005; Kobayashi & Kawakita 2009). $Q(H_2O)$ was usually derived as follows:

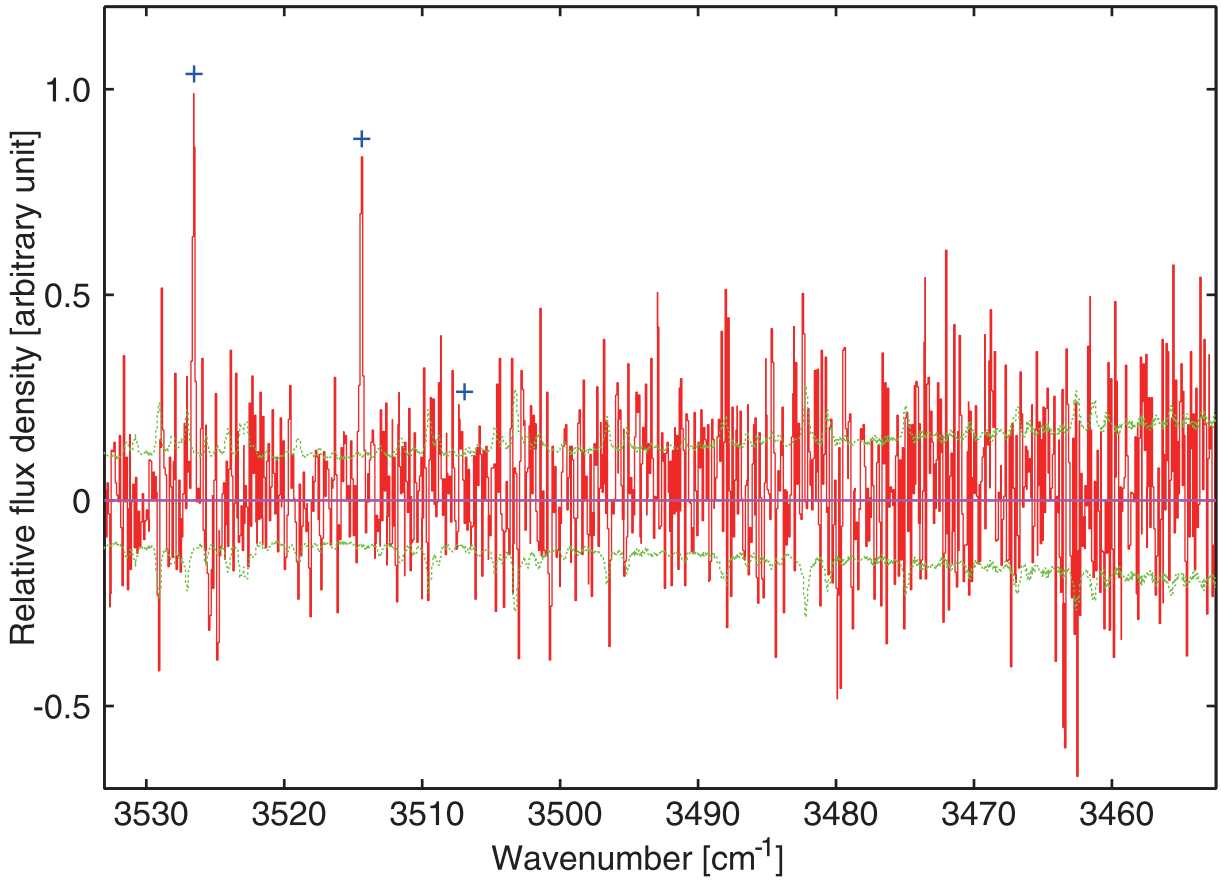


**Fig. 2.** One-dimensional spectrum of comet 46P/Wirtanen (red solid line). The "+" marks show the water emission lines. Green dotted lines show the $\pm 1\sigma$ errors.

$$Q(\mathrm{H_2O}) = \frac{4\pi\Delta^2}{f_{\mathrm{geom}}\,\tau_{\mathrm{H_2O}}}\frac{F_{\mathrm{H_2O}}}{g_{\mathrm{H_2O}}}, \quad (1)$$

where $\Delta$ denotes the geocentric distance [AU], $f_{\mathrm{geom}}$ the fraction of water molecules within the observed (slit) aperture, $\tau_{\mathrm{H_2O}}$ the photodissociation lifetime of $H_2O$ [s] ($8.3 \times 10^4$ s at 1 AU for the quiet Sun; see Huebner et al. 1992), $F_{\mathrm{H_2O}}$ the flux of $H_2O$ [W m$^{-2}$], and $g_{\mathrm{H_2O}}$ the $g$-factor (emission efficiency) [W molecule$^{-1}$]. We have to use the $g$-factor including the transmittance of the atmosphere. The transmittance curve is synthesized by the line-by-line radiative transfer model (LBLRTM) code (Clough et al. 2005). The code requires some parameters, such as the atmospheric conditions (temperature, pressure, relative humidity), airmass of the target, and molecular species. In our region of interest (3530–3500 cm$^{-1}$), the transmittance is strongly affected by $H_2O$ ($CO_2$ also contributes, but not significantly). The calculated transmittances are also listed in table 1. Fraction $f_{\mathrm{geom}}$ was simply calculated by the following expression (Kawara et al. 1988; Kobayashi et al. 2007):

$$f_{\mathrm{geom}} = \frac{\Delta}{2v_{\mathrm{exp}}\tau_{\mathrm{H_2O}}}\left(\theta_1 \mathrm{arcsinh}\frac{\theta_2}{\theta_1} + \theta_2 \mathrm{arcsinh}\frac{\theta_1}{\theta_2}\right), \quad (2)$$

where $v_{\mathrm{exp}}$ denotes the expansion velocity of the molecules [km s$^{-1}$]; $\theta_1$ and $\theta_2$ denote the slit length and the slit width [rad], respectively. This formula is applicable to the case of $[\theta_1\Delta\,/\,(v_{\mathrm{exp}}\tau_{\mathrm{H_2O}})]$ and $[\theta_2\Delta\,/\,(v_{\mathrm{exp}}\tau_{\mathrm{H_2O}})] \ll 1$. We assumed the simple Haser model for the spatial distribution of $H_2O$ in the coma with the expansion velocity, $v_{\mathrm{exp}} = 0.8{\times}r_{\mathrm{h}}^{-0.5}$[m s$^{-1}$] ($r_{\mathrm{h}}$: the heliocentric distance of the comet). $F_{\mathrm{H_2O}}$ was obtained from the observed spectrum and $g_{\mathrm{H_2O}}$ was calculated by our fluorescence excitation model.

Since details of our fluorescence excitation model for $H_2O$ were described in other paper (Kawakita & Kobayashi 2009), we summarize our model briefly. We assumed that $H_2O$ molecules are pumped up from a rotational level in the ground-vibrational state to the upper ro-vibrational level by the solar radiation field, and then cascade down to the lower ro-vibrational level and then to the ground-vibrational state. The population distribution in the ground-vibrational state is assumed to follow the Boltzmann distribution as a function of the temperature. Usually this temperature is called the "rotational temperature". Our $H_2O$ fluorescence excitation model has two free parameters: one is the rotational temperature, $T_{\mathrm{rot}}$, and the other is the Ortho-to-Para abundance ratio, *OPR*. For molecules having more than two identical protons (each proton has a nuclear spin of 1/2), like $H_2O$, there are two (or more) spin states corresponding the different rotational ladders. In the case of $H_2O$, these two spin states are called the "ortho" state (the total nuclear spin quantum number of protons, $I = 1$) and the "para" state ($I = 0$). The *OPR* value is 3.0 at the high-temperature limit.

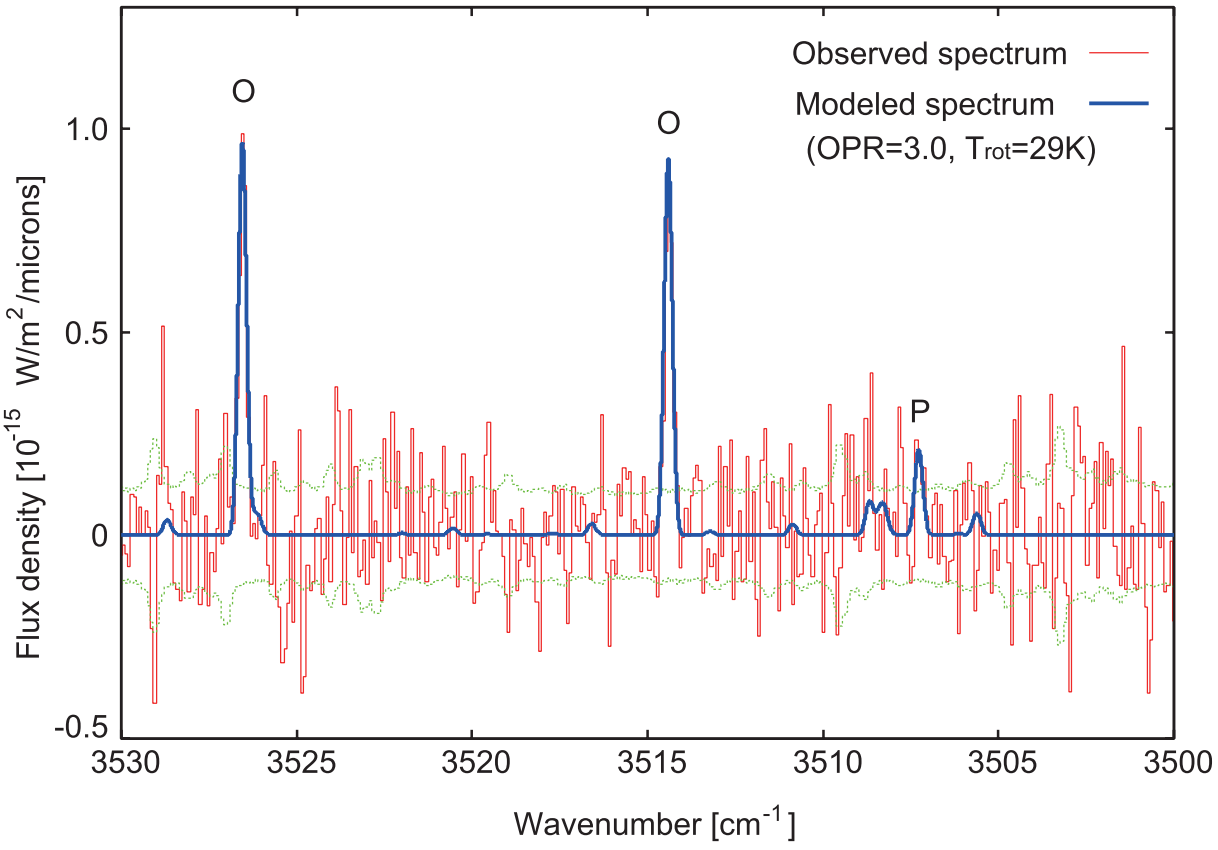


**Fig. 3.** One-dimensional observed spectrum of comet 46P/Wirtanen (thin red solid line) overlapped with the modeled spectrum (thick blue solid line) for $T_{\rm rot} = 36$ K and $OPR = 3.0$. The "O" and "P" marks indicate the "ortho" and "para" lines, respectively. The green dotted lines show the $\pm 1\,\sigma$ errors, as in figure 2.

We fitted the observed spectrum to the modeled spectrum, minimizing the reduced-$\chi^2$ to determine the best $T_{\rm rot}$ and $OPR$. We also adjusted the abundance of $H_2O$ in the upper telluric atmosphere to obtain the transmittances for the minimum reduced-$\chi^2$, although the atmospheric conditions at the ground level were fixed to the measured values during the period of comet observations. The best $OPR$ was determined to be $3.0^{+8.3}_{-1.4}$ (with $\pm 1\,\sigma$ errors). The $1\,\sigma$ error levels were determined based on the criterion of reduced-$\chi^2 \leq 1$. The errors of $OPR$ are very large and almost meaningless because of the small number of para lines (only a single para line could be detected, as listed in table 1). The obtained $OPR$ is consistent with the high-temperature limit (3.0) within the errors. Here we assumed $OPR$ to be 3.0. Thus, we fixed $OPR$ to be 3.0, and the best $T_{\rm rot}$ was determined to be $29^{+9}_{-6}$ K (with $\pm 1\,\sigma$ errors). The error levels were determined in the same way as the case of $OPR$. A comparison of the modeled spectrum with the observed spectrum is shown in figure 3. The $g$-factors (for $T_{\rm rot} = 29$ K and $OPR = 3.0$) are also listed in table 1.

When we determined the $Q(H_2O)$, "$Q$-curve analysis" is necessary to the conversion of the "nucleocentric" $Q(H_2O)$ determined above into the (true) "terminal" $Q(H_2O)$ (DiSanti & Mumma 2008) (figure 4). The growth factor [terminal-$Q(H_2O)$ / nucleocentric-$Q(H_2O)$] was estimated to be $1.32 \pm 0.08$ and the nucleocentric-$Q(H_2O)$ was determined to be $(1.3 \pm 0.2) \times 10^{28}$. This nucleocentric-$Q(H_2O)$ was determined to be a weighted mean of 3 water lines listed in table 1. The derived terminal-$Q(H_2O)$ is $(1.7 \pm 0.2) \times 10^{28}$ molecules s$^{-1}$. The errors correspond to $1\,\sigma$ levels that include the errors of the growth factor ($\sim$6%), $g$-factor ($\sim$5%), flux measurement ($\sim$10%), and $T_{\rm rot}$ ($\sim$5%).

Although uncertainty caused by changing atmospheric transmittance affects the determination of the water production rate, the influence is not considered to be significant. For example, we calculated the atmospheric transmittances with changing the scaling factors for the water abundance in the upper atmosphere relative to the standard vertical profile of water built in LBLRTM. Concerning a change of $\pm 20\%$ for the water abundance in the upper atmosphere (note that atmospheric conditions at the ground level were fixed in the calculation), the calculated transmittances at the interesting wavelengths are slightly different, but the resultant water production rates are within the error bars listed above, $(1.7 \pm 0.2) \times 10^{28}$.

## 4. Discussions and Conclusions

Although there are many reports on the water production rates of comet 46P in the 1997 apparition, there are no reports on the water production rates in the 2008 apparition. Fortunately, the cometary OH lines (OH is a photodissociation product of water) were observed with the Nançay radio telescope in the 2008 apparition (J. Crovisier 2009,

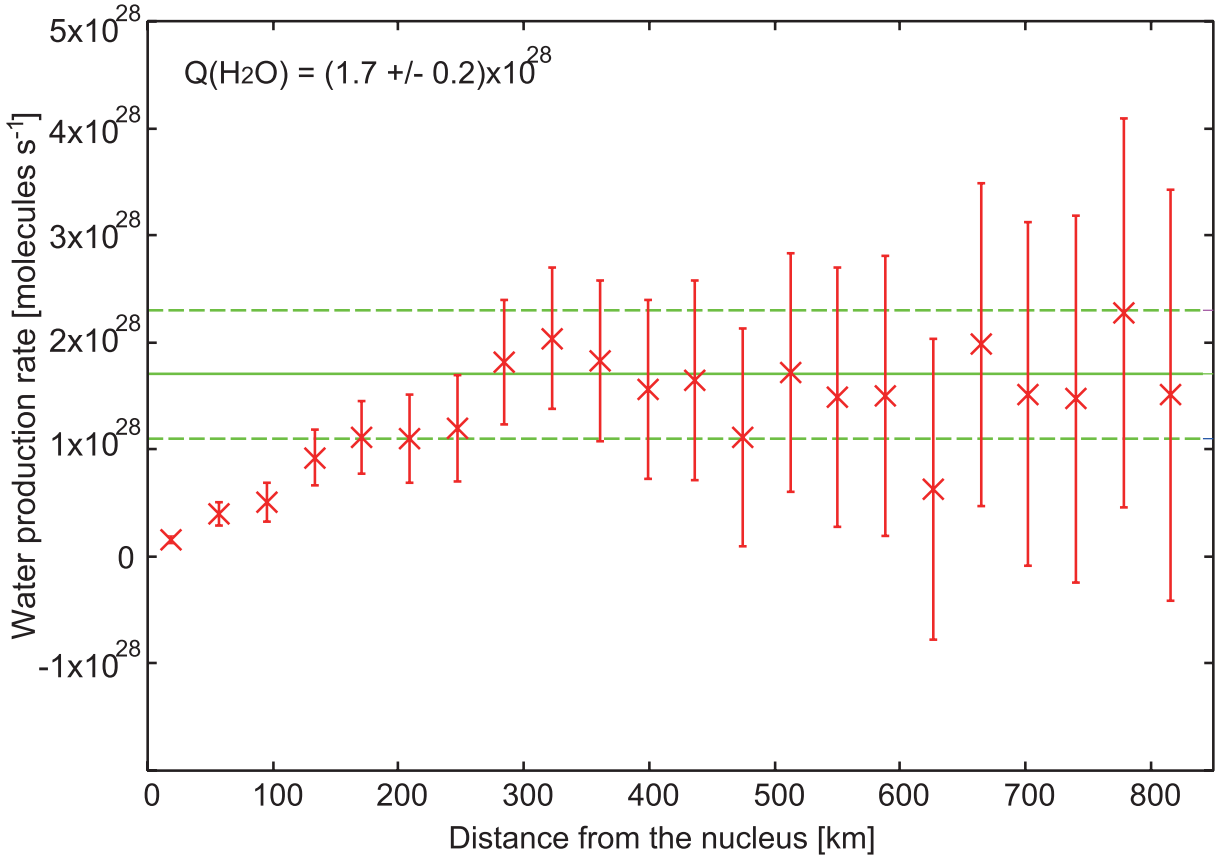


**Fig. 4.** "$Q$-curve analysis" for the water production rates. Each data point shows the water production rate at the distance from the nucleus determined by the spatial distribution of the water emission lines. The green (horizontal) lines show the "terminal $Q$ value" (solid) and the $3\sigma$ error levels (dashed).

private communication); we thus compare our result with his result (see table 2). The radio observations were carried out in comet 46P over the period of 2008 January 3–21 (pre-perihelion), and the averaged OH production rate was determined to be $(0.9 \pm 0.2) \times 10^{28}$ molecules $s^{-1}$ at $\sim 1.09$ AU (averaged heliocentric distance during the period from 2008 January 3 to 21). The reader could refer to Crovisier et al. (2002) for details on the Nançay observations and the derivation of $Q$(OH). To convert the OH production rate to the water production rate, we have to divide the OH production rate by its branching ratio from water (we used 0.85 as Fink & Combi 2004 did). The water production rate was calculated by the OH production rate as $(1.1 \pm 0.2) \times 10^{28}$ molecules $s^{-1}$ over the period of 2008 Janurary 3–21. Although our production rate is slightly larger than $Q(H_2O)$ derived from radio observations, they are consistent in value within $\pm 2\sigma$ errors. Both their radio and our infrared observations were carried out at similar heliocentric distances (this work: $r_h = 1.08$ AU in pre-perihelion; Crovisier's: averaged $r_h \sim 1.09$ AU in post-perihelion). Thus, we can conclude that there is no difference in activity between pre- and post-perihelion passages during the 2008 apparition of comet 46P. In previous apparitions, there was also no activity difference between pre- and post-perihelion passages (Fink & Combi 2004; Farnham & Schleicher 1998). Although there might be a slight evolution of the orbit of comet 46P (e.g., the perihelion distance changed by $\sim 0.02$ AU, from 1.083 AU in the 1991 apparition to 1.064 AU in the 1997 apparition while the perihelion distance in the 2008 apparition was 1.058 AU, which only varied by $\sim 0.01$ AU since the 1997 apparition), such an effect did not significantly affect the cometary activity in this case.

Additionally, in the light curve of the visual magnitude of comet 46P in the 2008 apparition (provided by S. Yoshida),[2] one can find that the light curve is asymmetric with respect to the perihelion passage after considering differences in the geocentric distances. However, both the reflected sunlight and the $C_2$ emission (the Swan band) contribute to the visual magnitude of a comet, and the visual magnitude is not a direct measure of $Q(H_2O)$. Actually, although the visual light curve in the 1997 apparition was asymmetric with respect to the perihelion passage, the curve of the water production rates was symmetric in the same apparition, as mentioned above. From the viewpoint of $Af\rho$, the sudden change of $Af\rho$ in the pre-perihelion passage reported by Schulz et al. (1998) might have been an outburst in the 1997 apparition (Stern et al. 1998). Note that there was no hint of the outburst in the light curve of the visual magnitude in the 2008 apparition (provided by S. Yoshida).[2]

When we compare the production rates (or abundance ratios) derived from the radio observation with those from near-infrared one, we have to consider the differences in the field

[2] ⟨http://www.aerith.net/comet/catalog/0046P/⟩.

**Table 2.** Summary of water production rates of comet 46P/Wirtanen.

| Observation date [UT] | $r_h$ [AU] | Water production rate* [molecules $s^{-1}$] | Corrected water production rate† [molecules $s^{-1}$] | Remarks | Reference‡ |
|---|---|---|---|---|---|
| **2008 apparition** | **pre-perihelion** | | | | |
| 2008 Jan 3–21 | 1.09 | $(1.1 \pm 0.2) \times 10^{28}$ | $(1.1 \pm 0.2) \times 10^{28}$ | OH, radio, averaged | [1] |
| **2008 apparition** | **post-perihelion** | | | | |
| 2008 Feb 19 | 1.08 | $(1.7 \pm 0.2) \times 10^{28}$ | $(1.8 \pm 0.2) \times 10^{28}$ | $H_2O$, NIR | This work |
| **1997 apparition** | **pre-perihelion** | | | | |
| 1996 Aug 26 | 2.47 | | $(2.7 \pm 0.5) \times 10^{26}$ | OH, mid UV | [2] |
| 1996 Dec 21 | 1.52 | | $(9.6 \pm 2.4) \times 10^{26}$ | Ly$\alpha$ | [3] |
| 1996 Dec 23 | 1.50 | | $(3.7 \pm 0.9) \times 10^{26}$ | Ly$\alpha$ | [3] |
| 1996 Dec 28 | 1.46 | | $(3.0 \pm 0.8) \times 10^{27}$ | Ly$\alpha$ | [3] |
| 1996 Dec 30 | 1.44 | | $(5.9 \pm 1.5) \times 10^{27}$ | Ly$\alpha$ | [3] |
| 1997 Jan 1 | 1.43 | | $(9.2 \pm 2.3) \times 10^{27}$ | Ly$\alpha$ | [3] |
| 1997 Jan 4 | 1.40 | | $(8.3 \pm 2.1) \times 10^{27}$ | Ly$\alpha$ | [3] |
| 1997 Jan 8 | 1.37 | | $(1.0 \pm 0.3) \times 10^{28}$ | Ly$\alpha$ | [3] |
| 1997 Jan 10 | 1.36 | | $(6.5 \pm 1.6) \times 10^{27}$ | Ly$\alpha$ | [3] |
| 1997 Jan 15 | 1.31 | | $(5.1 \pm 0.3) \times 10^{26}$ | OH, mid UV | [2] |
| 1997 Jan 23 | 1.26 | | $(1.1 \pm 0.3) \times 10^{28}$ | Ly$\alpha$ | [3] |
| 1997 Jan 24 | 1.26 | | $(1.0 \pm 0.3) \times 10^{28}$ | Ly$\alpha$ | [3] |
| 1997 Jan 25 | 1.25 | | $(9.5 \pm 2.4) \times 10^{27}$ | Ly$\alpha$ | [3] |
| 1997 Jan 30 | 1.22 | | $(7.5 \pm 1.9) \times 10^{27}$ | Ly$\alpha$ | [3] |
| 1997 Jan 31 | 1.21 | | $(9.5 \pm 2.4) \times 10^{27}$ | Ly$\alpha$ | [3] |
| 1997 Feb 3 | 1.20 | | $(9.8 \pm 2.4) \times 10^{27}$ | Ly$\alpha$ | [3] |
| 1997 Jan 18–Feb 4 | 1.19 | | $(1.6 \pm 0.4) \times 10^{28}$ | [O I], optical | [4] |
| 1997 Feb 7 | 1.17 | | $(9.5 \pm 2.4) \times 10^{27}$ | Ly$\alpha$ | [3] |
| 1997 Feb 10 | 1.16 | | $(1.1 \pm 0.3) \times 10^{28}$ | Ly$\alpha$ | [3] |
| 1997 Feb 12 | 1.14 | | $(1.5 \pm 0.5) \times 10^{28}$ | Ly$\alpha$ | [3] |
| 1997 Feb 13 | 1.14 | | $(8.9 \pm 2.2) \times 10^{27}$ | Ly$\alpha$ | [3] |
| 1997 Feb 14 | 1.14 | | $(1.1 \pm 0.3) \times 10^{28}$ | Ly$\alpha$ | [3] |
| 1997 Feb 15 | 1.14 | | $(1.4 \pm 0.3) \times 10^{28}$ | Ly$\alpha$ | [3] |
| 1997 Feb 15 | 1.13 | | $(1.4 \pm 0.4) \times 10^{28}$ | Ly$\alpha$ | [3] |
| 1997 Feb 15 | 1.13 | | $(1.5 \pm 0.2) \times 10^{28}$ | OH, optical | [5] |
| 1997 Feb 17 | 1.13 | | $(1.1 \pm 0.3) \times 10^{28}$ | Ly$\alpha$ | [3] |
| 1997 Feb 4 and Mar 5 | 1.12 | $< 1.8 \times 10^{28}$ | $< 1.9 \times 10^{28}$ | OH, radio, averaged | [6] |
| 1997 Feb 22 | 1.11 | | $(1.6 \pm 0.4) \times 10^{28}$ | Ly$\alpha$ | [3] |
| 1997 Feb 24 | 1.10 | | $(1.6 \pm 0.4) \times 10^{28}$ | Ly$\alpha$ | [3] |
| 1997 Feb 28 | 1.09 | | $(1.7 \pm 0.4) \times 10^{28}$ | Ly$\alpha$ | [3] |
| 1997 Mar 1 | 1.09 | | $(1.6 \pm 0.4) \times 10^{28}$ | Ly$\alpha$ | [3] |
| 1997 Mar 3 | 1.08 | | $(1.7 \pm 0.4) \times 10^{28}$ | Ly$\alpha$ | [3] |
| 1997 Mar 6 | 1.08 | | $(1.5 \pm 0.4) \times 10^{28}$ | Ly$\alpha$ | [3] |
| 1997 Mar 7 | 1.08 | | $(1.6 \pm 0.4) \times 10^{28}$ | Ly$\alpha$ | [3] |
| 1997 Mar 8 | 1.08 | | $(1.4 \pm 0.4) \times 10^{28}$ | Ly$\alpha$ | [3] |
| 1997 Mar 2–6 | 1.07 | | $(1.4 \pm 0.6) \times 10^{28}$ | [O I], optical | [4] |
| 1997 Mar 10 | 1.07 | | $(1.6 \pm 0.4) \times 10^{28}$ | Ly$\alpha$ | [3] |
| 1997 Mar 13 | 1.07 | | $(1.5 \pm 0.4) \times 10^{28}$ | Ly$\alpha$ | [3] |
| **1997 apparition** | **post-perihelion** | | | | |
| 1997 Mar 29–Apr 2 | 1.08 | | $(1.9 \pm 0.5) \times 10^{28}$ | [O I], optical | [4] |
| 1997 Mar 22 | 1.08 | | $(1.4 \pm 0.4) \times 10^{28}$ | Ly$\alpha$ | [3] |
| 1997 Mar 23 | 1.08 | | $(5.9 \pm 1.5) \times 10^{27}$ | Ly$\alpha$ | [3] |
| 1997 Mar 25 | 1.08 | | $(1.4 \pm 0.3) \times 10^{28}$ | Ly$\alpha$ | [3] |
| 1997 Apr 1 | 1.10 | | $(2.3 \pm 0.6) \times 10^{28}$ | Ly$\alpha$ | [3] |
| 1997 Apr 29–May 3 | 1.24 | | $(6.0 \pm 0.2) \times 10^{27}$ | [O I], optical | [4] |
| 1997 May 1 | 1.24 | | $(3.7 \pm 0.9) \times 10^{27}$ | Ly$\alpha$ | [3] |
| 1997 May 2 | 1.25 | | $(2.5 \pm 0.6) \times 10^{27}$ | Ly$\alpha$ | [3] |
| 1997 May 4 | 1.26 | | $(3.2 \pm 0.8) \times 10^{27}$ | Ly$\alpha$ | [3] |

**Table 2.** (Continued)

| Observation date [UT] | $r_h$ [AU] | Water production rate* [molecules $s^{-1}$] | Corrected water production rate† [molecules $s^{-1}$] | Remarks | Reference‡ |
|---|---|---|---|---|---|
| 1997 May 5 | 1.26 | | $(6.3 \pm 1.6) \times 10^{27}$ | Ly$\alpha$ | [3] |
| 1997 May 7 | 1.28 | | $(6.7 \pm 1.7) \times 10^{27}$ | Ly$\alpha$ | [3] |
| 1997 May 9 | 1.29 | | $(5.2 \pm 1.3) \times 10^{27}$ | Ly$\alpha$ | [3] |
| 1997 May 10 | 1.30 | | $(7.6 \pm 1.9) \times 10^{27}$ | Ly$\alpha$ | [3] |
| 1997 May 12 | 1.31 | | $(3.1 \pm 0.8) \times 10^{27}$ | Ly$\alpha$ | [3] |
| 1997 May 14 | 1.33 | | $(3.4 \pm 0.9) \times 10^{27}$ | Ly$\alpha$ | [3] |
| 1997 May 17 | 1.35 | | $(9.9 \pm 2.5) \times 10^{27}$ | Ly$\alpha$ | [3] |
| 1997 Jun 1–2 | 1.47 | | $(2.2 \pm 1.8) \times 10^{27}$ | [O I], optical | [4] |

* Using $v_{exp} = 0.85 \times r_h^{-0.5}$.

† Using $v_{exp} = 0.80 \times r_h^{-0.5}$ based on Fink and Combi (2004).

‡ [1] J. Crovisier (2009, private communication), [2] Stern et al. (1998), [3] Bertaux et al. (1999), [4] Fink et al. (1998), [5] Farnham and Schleicher (1998), [6] Crovisier et al. (2002).

of view (FOV) between these observations. Usually, the FOV of radio observations is much wider than that of near-infrared observations. For our observations we have to extrapolate the total water production rate based on measurements in a very narrow aperture region. On the other hand, radio observations can cover a large part of the coma of OH, and they need minimal extrapolations to determine the total OH production rate. For an optical study, we note that the water production rates depend on the spatial-distribution model of the coma than the FOV for comet 46P (Fink & Combi 2004).

We note that photodissociation lifetime of OH at 1 AU ($1.6 \times 10^5$ s) used in Crovisier et al. (2002) is different from the experimental values listed in Huebner, Keady, and Lyon (1992), $5 \times 10^4$ s for the quiet Sun condition and $2.9 \times 10^4$ s for the active Sun. In the 2008 apparition, the solar activity was near minimum. Since the production rate of OH is proportional to the reciprocal of the lifetime of OH [$Q(\mathrm{OH}) \propto \tau_{\mathrm{OH}}^{-1}$], the $Q$(OH) [and $Q(H_2O)$] becomes larger if we use the lifetime of OH listed in Huebner, Keady, and Lyon (1992). This may affect the slight difference in the water production rates in the 2008 apparition.

We also compared our water production rate with those derived from many different observations in the 1997 apparition: Stern et al. (1998) by mid-UV spectroscopy (OH); Fink et al. (1998) by optical spectroscopy ([O I]); Bertaux et al. (1999) by UV imaging (Ly$\alpha$); Farnham and Schleicher (1998) by optical photometry (OH); Crovisier et al. (2002) by radio observations (OH). Fink and Combi (2004) summarized water production rates reported by different groups. These water production rates listed in Fink and Combi (2004) were corrected for differences in the scale lengths and the expansion velocities of both the parent and the daughter species ($v_{exp,parent} = 0.85 \times r_h^{-0.5}$ [km $s^{-1}$], $v_{exp,daughter} = 1.0$ km $s^{-1}$; parent scale length = $68000 \times r_h^{1.5}$ [km], daughter scale length = $160000 \times r_h^2$ [km]) in the different models used by different groups, where "parent" is $H_2O$ and "daughter" is OH. Expansion velocities of the parent molecule differ between ours ($v_{exp} = 0.8 \times r_h^{-0.5}$ [km $s^{-1}$]) and that used in Fink and Combi ($v_{exp,Fink\&Combi} = 0.85 \times r_h^{-0.5}$ [km $s^{-1}$]), i.e., ($v_{exp,Fink\&Combi}/v_{exp}$) $\sim$ 1.06. We scaled our water production rate with 1.06 to $Q_{cor} = (1.8 \pm 0.2) \times 10^{28}$ molecules $s^{-1}$.

We should note that the water production rate determined by Bertaux (1997) is not the same as Bertaux et al. (1999, renewal of 1997 results), as noted by the authors. Although Fink and Combi (2004) used the water production reported by Bertaux (1997), Bertaux et al. (1999) mentioned that water production rate listed in the 1997 report was faultily determined. Moreover, if we correct the water production rate determined by Ly$\alpha$, as done by Fink and Combi (2004), we have to know the scale lengths of the grandparent ($H_2O$), parent (OH), and daughter (H) species for the three-generation Haser model (e.g., Krishna Swamy 1997). Fink and Combi (2004) mentioned about the corrections only for the parent ($H_2O$) and the daughter (OH). Thus, we used the results of the water production rates determined from the Ly$\alpha$ observations listed in Bertaux et al. (1999) with no corrections for the scale lengths in this paper. Furthermore, Crovisier et al. (2002) used the expansion velocity of the parent ($0.8 \times r_h^{-0.5}$ [km $s^{-1}$]) to be the same as our value; the water production rates were also corrected as $(1.1 \pm 0.3) \times 10^{28}$ molecules $s^{-1}$ for the 2008 apparition, and as $< 1.9 \times 10^{28}$ molecules $s^{-1}$ for the 1997 apparition by using $v_{exp,Fink\&Combi} = 0.85 \times r_h^{-0.5}$ [km $s^{-1}$].

We summarize these corrected water production rates in table 2 and figure 5. We fitted the water production rate obtained from the data in the 1997 apparition by a power law ($r_h^{-n}$), and the best slope was determined to be $n = 5.7 \pm 0.5$ (with $1\sigma$ errors). This value is consistent with the slopes determined in other studies [e.g., $-4.3$ (Fink & Combi 2004); $\sim -4$ (Farnham & Schleicher 1998); $-4.9$ (Bertaux et al. 1999); $-4.9 \pm 0.25$ (Stern et al. 1998)] within $\pm 3\sigma$ errors. We note that the fitted $r_h$ slope shown in figure 5 is drawn with $\pm 3\sigma$ errors for the 1997 apparition. We did not determine the slope of the data in the 2008 apparition because there were only two observational points, and those data were observed very close to $r_h$ (1.08 and 1.09 AU). The water production rates determined in the 2008 apparition are also shown in figure 5; these results are certainly suited for the slope determined by the 1997 observations within $\pm 3\sigma$ errors. This result implies that the trend of the water production rates is similar to those in different apparitions of 1991–2008, as Farnham and Schleicher (1998) pointed out for the 1991 and 1997 apparitions. Thus, for comet 46P, we conclude that there have been no secular variations in the water production rate in recent decades, at

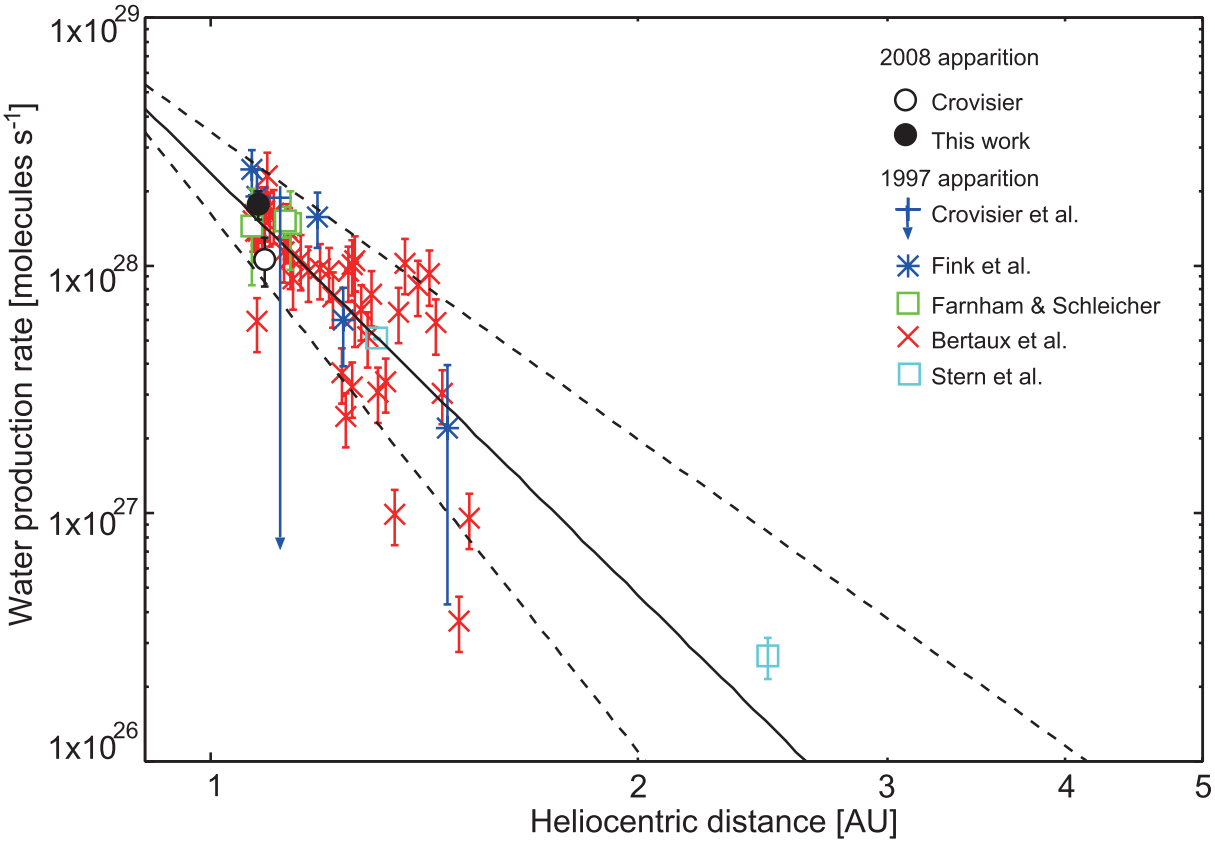


**Fig. 5.** Water production rates determined by different observations in the 2008 apparition (black and white) and 1997 apparition (in color). We fitted the water production rates in the 1997 apparition data by a power law ($r_h^{-n}$). The best-fit slope, determined to be $n = 5.7$, is shown by the black solid line. The black dashed lines correspond to the $\pm 3\sigma$ errors of the best fit (see text).

least around the perihelion passage, even though the orbit of the comet has been slightly changed. We hope that additional observations will be carried out in future apparitions to determine the water production rates in comet 46P.

The authors thank J. Crovisier for providing his results prior to the publication. We are also grateful to B. Bonev for his valuable comments and suggestions. This research is based on data collected at Subaru Telescope, which is operated by the National Astronomical Observatory of Japan. This research is supported by the Research Fellow of Japan Society of the Promotion of Science (H. Kobayashi).

## References

A'Hearn, M. F., Millis, R. L., Schleicher, D. G., Osip, D. J., & Birch, P. V. 1995, Icarus, 118, 223
Bertaux, J.-L. 1997, IAU Circ., 6565
Bertaux, J. L., Costa, J., Mäkinen, T., Quémerais, E., Lallement, R., Kyrölä, E., & Schmidt, W. 1999, Planet. Space Sci., 47, 725
Bockelée-Morvan, D., Crovisier, J., Mumma, M. J., & Weaver, H. A. 2004, in Comets II, ed. M. C. Festou et al. (Tucson: University of Arizona Press), 391
Clough, S. A., Shephard, M. W., Mlawer, E. J., Delamere, J. S., Iacono, M. J., Cady-Pereira, K., Boukabara, S., & Brown, P. D. 2005, J. Quant. Spectrosc. Radiat. Transfer, 91, 233
Crovisier, J., Colom, P., Gérard, E., Bockelée-Morvan, D., & Bourgois, G. 2002, A&A, 393, 1053
Dello Russo, N., Bonev, B. P., DiSanti, M. A., Mumma, M. J., Gibb, E. L., Magee-Sauer, K., Barber, R. J., & Tennyson, J. 2005, ApJ, 621, 537
Dello Russo, N., DiSanti, M. A., Magee-Sauer, K., Gibb, E. L., Mumma, M. J., Barber, R. J., & Tennyson, J. 2004, Icarus, 168, 186
DiSanti, M. A., & Mumma, M. J. 2008, Space Sci. Rev., 138, 127
Farnham, T. L., & Schleicher, D. G. 1998, A&A, 335, L50
Fink, U., & Combi, M. R. 2004, Planet. Space Sci., 52, 573
Fink, U., Hicks, M. D., Fevig, R. A., & Collins, J. 1998, A&A, 335, L37
Huebner, W. F., Keady, J. J., & Lyon, S. P. 1992, Ap&SS, 195, 1
Jockers, K., Credner, T., & Bonev, T. 1998, A&A, 335, L56
Kawakita, H., & Kobayashi, H. 2009, ApJ, 693, 388
Kawara, K., Gregory, B., Yamamoto, T., & Shibai, H. 1988, A&A, 207, 174
Kobayashi, H., & Kawakita, H. 2009, ApJ, 703, 121
Kobayashi, H., Kawakita, H., Mumma, M. J., Bonev, B. P., Watanabe, J., & Fuse, T. 2007, ApJ, 668, L75

Kobayashi, N., et al. 2000, Proc. SPIE, 4008, 1056
Krishna Swamy, K. S. 1997, Physics of Comets, 2nd ed. (Singapore: World Science Publishing), 131
Lamy, P. L., Toth, I., Jorda, L., Weaver, H. A., & A'Hearn, M. 1998, A&A, 335, L25
Mäkinen, J. T. T., Bertaux, J.-L., Pulkkinen, T. I., Schmidt, W., Kyrölä, E., Summanen, T., Quémerais, E., & Lallement, R. 2001, A&A, 368, 292
Schulz, R., Arpigny, C., Manfroid, J., Stüwe, J. A., Tozzi, G. P., Rembor, K., Cremonese, G., & Peschke, S. 1998, A&A, 335, L46
Stern, S. A., et al. 1998, A&A, 335, L30